Volume 9, Number 12
1009-1963/2000/09(12)/0900-05
CHINESE PHYSICS
December, 2000
© 2000 Chin. Phys. Soc.

# SPECTRUM OF THE MICROMASER INJECTED WITH $\Lambda$-TYPE THREE-LEVEL ATOMS

Zhang Zhi-ming(张智明), Liang Wen-Qing(梁文青), Xie Sheng-wu(谢绳武)
*Department of Applied Physics, Shanghai Jiao Tong University, Shanghai* 200240, *China*

(Received 1 February 2000; revised manuscript received 2 July 2000)

The spectrum of the micromaser injected with $\Lambda$-type three-level atoms is studied. The spectrum has a Lorentzian lineshape and its central frequency has a shift. The effects of various parameters (for example, the atomic center-of-mass velocity, the cavity-length, the one-photon detuning, the ratio of the atomic injection rate to the cavity decay rate and the number of thermal photons) on the linewidth and the frequency shift are examined. The spectrum shows very different features in different velocity regimes, i.e., in the fast-atom regime, in the intermediate-velocity-atom regime, and in the slow-atom regime.

**Keywords:** micromaser, $\Lambda$-type three-level atom, spectrum
**PACC:** 4250

## I. INTRODUCTION

Micromaser plays an important role in the study of cavity quantum electrodynamics.[1] On the other hand, with the development of laser cooling techniques,[2] one has obtained very cold atoms (ultracold atoms). Recently, Scully, Meyer and Walther[3] suggested to use the ultracold atoms in micromaser studies and proposed the concept of the mazer (Microwave Amplification via $Z$-motion-induced Emission of Radiation).They and their coworkers have studied many properties, for example, the emission probability, the photon statistics and the spectrum, of the mazer in a series of papers.[4–6] However, the two-level atom model was assumed in their papers. More recently, we have studied the emission probability[7] and the photon statistics[8] in the micromaser injected with ultracold $\Lambda$-type three-level atoms. In the present paper we study the spectrum of this system.

## Ⅱ. MASTER EQUATION

Suppose that the atom has a $\Lambda$-type three-level configuration (Fig.1), moves along the $z$-direction, and enters into a cavity which contains a single-mode quantum radiation field. We suppose that, initially, the atom is in the upper state $|a\rangle$ and with a center-of-mass momentum $k(\hbar = 1)$ and the cavity field is in a superposition state $\sum_n C_n|n\rangle$. In Ref.[8] we have derived the following master equation for the reduced density matrix of the cavity field

$$\dot{\rho}_{nm} = a_{nm}\rho_{nm} + b_{n-1,m-1}\rho_{n-1,m+1} + c_{n+1,m+1}\rho_{n+1,m+1}, \tag{1}$$

where

$$a_{nm} = r_a[(R_{a,n}R^*_{a,m} + T_{a,n}T^*_{a,m}) - 1] - \frac{\gamma}{2}(n_b+1)(n+m) - \frac{\gamma}{2}n_b(n+m+2), \tag{2a}$$

$$b_{nm} = r_a[(R_{b,n+1}R^*_{b,m+1} + T_{b,n+1}T^*_{b,m+1}) + (R_{c,n+1}R^*_{c,m+1} + T_{c,n+1}T^*_{c,m+1})] + \gamma n_b\sqrt{(n+1)(m+1)}, \tag{2b}$$

$$c_{nm} = \gamma(n_b+1)\sqrt{nm}, \tag{2c}$$

in which $r_a$ is the atomic injection rate, $\gamma$ is the cavity decay rate, $n_b$ is the number of photons in thermal equilibrium, and

$$R_{a,n}(k) = \frac{1}{2\Omega_n}\left[\left(\Omega_n + \frac{\Delta}{2}\right)\rho^+_n(k) + \left(\Omega_n - \frac{\Delta}{2}\right)\rho^-_n(k)\right], \tag{3a}$$

$$T_{a,n}(k) = \frac{1}{2\Omega_n}\left[\left(\Omega_n + \frac{\Delta}{2}\right)\tau^+_n(k) + \left(\Omega_n - \frac{\Delta}{2}\right)\tau^-_n(k)\right], \tag{3b}$$

$$R_{b,n+1}(k) = \frac{d_1(n)}{2\Omega_n}[\rho^+_n(k) - \rho^-_n(k)], \tag{3c}$$

$$T_{b,n+1}(k) = \frac{d_1(n)}{2\Omega_n}[\tau^+_n(k) - \tau^-_n(k)], \tag{3d}$$

$$R_{c,n+1}(k) = \frac{d_2(n)}{2\Omega_n}[\rho^+_n(k) - \rho^-_n(k)], \tag{3e}$$

$$T_{c,n+1}(k) = \frac{d_2(n)}{2\Omega_n}[\tau^+_n(k) - \tau^-_n(k)], \tag{3f}$$

with

$$\Omega_n = \sqrt{\left(\frac{\Delta}{2}\right)^2 + G_n^2},$$
$$G_n = \sqrt{d_1^2(n) + d_2^2(n)},$$
$$d_i(n) = g_i\sqrt{n+1}, \tag{4}$$

where $\Delta$ is the one-photon detuning between the cavity field frequency and the atomic transition frequency, $g_1$ ($g_2$) is the coupling constant between the field and the atomic transition $|a\rangle \leftrightarrow |b\rangle$ ($|a\rangle \leftrightarrow |c\rangle$). $\rho_n^{\pm}(k)$ and $\tau_n^{\pm}(k)$ are the reflection and transmission coefficients for the positive and negative components[7,8], respectively.

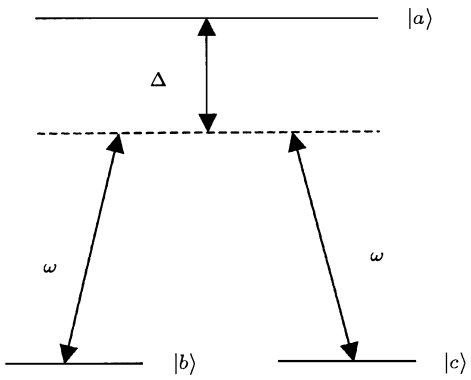



**Fig.1.** Schematic diagram of the Λ-type three-level atom interacting with a single-mode radiation field.

The meanings of $R's$ and $T's$ are as follows: When an atom, initially in the state $|a\rangle$, enters into a cavity containing $n$ photons, it may be reflected or transmitted while remaining in the state $|a\rangle$ with the amplitudes $R_{a,n}$ and $T_{\mathrm{a,n}}$; it may also be reflected or transmitted while making a transition to the state $|x\rangle$ ($x = b, c$) and emitting one photon with the amplitudes $R_{x,n+1}$ and $T_{x,n+1}$, respectively.

If the atom-field coupling inside the cavity along the $z$-direction is a constant, then the reflection and transmission coefficients $\rho_n^{\pm}(k)$ and $\tau_n^{\pm}(k)$ can be calculated analytically and have the following forms[7,8]

$$\rho_n^{\pm} = i\Delta_n^{\pm}\sin(K_n^{\pm}l)\tau_n^{\pm}, \tag{5}$$
$$\tau_n^{\pm} = [\cos(K_n^{\pm}l) - i\Sigma_n^{\pm}\sin(K_n^{\pm}l)]^{-1}, \tag{6}$$

where

$$K_n^{\pm} = \sqrt{k^2 \mp (k_n^{\pm})^2},$$
$$k_n^{\pm} = \sqrt{2M\left(\Omega_n \pm \frac{\Delta}{2}\right)}, \tag{7}$$

$$\Delta_n^{\pm} = \frac{1}{2}\left(\frac{K_n^{\pm}}{k} - \frac{k}{K_n^{\pm}}\right),$$
$$\Sigma_n^{\pm} = \frac{1}{2}\left(\frac{K_n^{\pm}}{k} + \frac{k}{K_n^{\pm}}\right), \tag{8}$$

in which $l$ is the cavity-length and $M$ is the atomic mass. Note that in the case of $k = k_n^+$, i.e., $K_n^+ = 0$, Eqs.(5) and (6) with (7) and (8) are not valid for the plus (+) components, in this case we find

$$\rho_n^+ = \frac{-ik_n^+ l}{2 - ik_n^+ l}, \quad \tau_n^+ = \frac{2}{2 - ik_n^+ l}. \tag{9}$$

Equation (1) is an important equation which can be used to study many properties of the cavity field. By using its diagonal elements we have studied the photon statistics in Ref.[8]. In this paper we study the spectrum of the field by using its off-diagonal elements.

## Ⅲ. SPECTRUM

The spectrum is governed by the decay of the expectation value of the electric field[9]

$$< E^{(-)}(t) > \sim < a^+(t) > = \sum_{n=0}^{\infty}\sqrt{n+1}\rho_{n,n+1}(t). \tag{10}$$

We see that the spectrum is different from the steady-state photon statistics[8] in two respects: (i) it involves the off-diagonal elements $\rho_{n,n+1}(t)$ of the reduced density matrix of the field, and (ii) it requires the full time dependence rather than the steady-state values. Equation (1) can be rewritten as

$$\dot{\rho}_n^{(k)}(t) = a_n^{(k)}\rho_n^{(k)} + b_{n-1}^{(k)}\rho_{n-1}^{(k)} + c_{n+1}^{(k)}\rho_{n+1}^{(k)}, \tag{11}$$

where $y_n^{(k)}(y = \rho, a, b, c)$ stands for $y_{n,n+k}$. Supposing that

$$\rho_n^{(k)}(t) = \exp[-\varphi_n^{(k)}(t)]\rho_n^{(k)}(0), \tag{12}$$

then from Eq.(11) we get

$$\begin{aligned}-\dot{\varphi}_n^{(k)}(t) =& a_n^{(k)} + [\rho_n^{(k)}(0)]^{-1} \\ &\times \{\exp[\varphi_n^{(k)}(t) - \varphi_{n-1}^{(k)}(t)]b_{n-1}^{(k)}\rho_{n-1}^{(k)}(0) \\ &+ \exp[\varphi_n^{(k)}(t) - \varphi_{n+1}^{(k)}(t)]c_{n+1}^{(k)}\rho_{n+1}^{(k)}(0)\}.\end{aligned} \tag{13}$$

Now we assume that[9]

$$|\varphi_n^{(k)}(t) - \varphi_{n\pm1}^{(k)}(t)| << 1, \tag{14}$$

and

$$[b_{n-1}^{(k)}\rho_{n-1}^{(k)}(0)+c_{n+1}^{(k)}\rho_{n+1}^{(k)}(0)] =[b_n^{(k)}+c_n^{(k)}][\rho_n^{(k)}(0)]. \quad (15)$$

Equation (14) leads to $\exp[\varphi_n^{(k)}(t)-\varphi_{n\pm1}^{(k)}(t)]\approx 1$ and Eq.(15) corresponds to the detailed balance condition $c_{n+1}^{(k)}\rho_{n+1}^{(k)}(0)=b_n^{(k)}\rho_n^{(k)}(0)$ in Ref.[9]. Under these two conditions, Eq.(13) can be reduced to

$$\dot{\varphi}_n^{(k)}(t)\approx\frac{1}{2}\mu_n^{(k)}, \quad (16)$$

and its solution is

$$\varphi_n^{(k)}(t)=\frac{1}{2}\mu_n^{(k)}t, \quad (17)$$

where

$$\frac{1}{2}\mu_n^{(k)}\equiv-(a_n^{(k)}+b_n^{(k)}+c_n^{(k)}). \quad (18)$$

Substituting Eq.(17) with $k=1$ into Eq.(12), and in turn, into Eq.(10), we get

$$< a^+(t) >=\sum_{n=0}^{\infty}\sqrt{n+1}\exp\left[-\frac{1}{2}\mu_n^{(1)}t\right]\rho_n^{(1)}(0) \approx\exp\left[-\frac{1}{2}<\mu_n^{(1)}>t\right]\sum_{n=0}^{\infty}\sqrt{n+1}\rho_n^{(1)}(0), \quad (19)$$

where

$$<\mu_n^{(1)}>=\sum_{n=0}^{\infty}\mu_n^{(1)}P_n, \quad (20)$$

in which $P_n$ is the steady-state photon number distribution, which has been found in Ref.[8]. It has the following form

$$P_n=P_0\prod_{m=1}^{n}X_m, \quad (21)$$

where $P_0$ is the normalized constant

$$P_0=\left[1+\sum_{n=1}^{\infty}\prod_{m=1}^{n}X_m\right]^{-1}, \quad (22)$$

and

$$X_m=\frac{1}{n_b+1}\left[n_b+\frac{N_{\rm ex}}{m}P_{\rm ems}(m-1)\right],(m\geq 1) \quad (23)$$

in which $N_{\rm ex}=r_a/\gamma$ is the number of atoms injected into the cavity during the cavity lifetime (or simply, the normalized injection rate) and

$$P_{\rm ems}(n)=|R_{b,n+1}(k)|^2+|T_{b,n+1}(k)|^2 +|R_{c,n+1}(k)|^2+|T_{c,n+1}(k)|^2 \quad (24)$$

is the emission probability.[7]

In general, $<\mu_n^{(1)}>$ is a complex number, i.e. $<\mu_n^{(1)}>=\mathrm{Re}<\mu_n^{(1)}>+i\mathrm{Im}<\mu_n^{(1)}>$. Substituting this into Eq.(19) and making Fourier transform we get the spectrum

$$\begin{aligned}F(\omega-\omega_c)&\propto\int \mathrm{d}t\exp\{-i(\omega-\omega_c)t\}<a^+(t)>\\ &\propto\int \mathrm{d}t\exp\{-i(\omega-\omega_c)t\}\\ &\times\exp\Big[-\frac{1}{2}<\mu_n^{(1)}>t\Big]\\ &\propto\int \mathrm{d}t\exp\Big\{\Big\{-i\Big[\omega-\Big(\omega_c\\ &-\frac{1}{2}\mathrm{Im}<\mu_n^{(1)}>\Big)\Big]\\ &-\frac{1}{2}\mathrm{Re}<\mu_n^{(1)}>\Big\}t\Big\},\end{aligned} \quad (25)$$

where $\omega_c$ is the cavity frequency. Equation(25) leads to a Lorentzian lineshape with a linewidth $\mathrm{Re}<\mu_n^{(1)}>$ centered at $(\omega_c-\mathrm{Im}<\mu_n^{(1)}>/2)$. That is, the central frequency has a shift $(-\mathrm{Im}<\mu_n^{(1)}>/2)$ from the cavity frequency $\omega_c$. In order to examine the properties of $<\mu_n^{(1)}>$ in more detail, we have done numerical calculations and drawn Figs.2–4. In the numerical calculations we have introduced $\eta=g_2/g_1(\eta=0$ corresponds to the two-level case) and $\kappa=\sqrt{2Mg_1}$; $\kappa$ has the dimension of a momentum (note $\hbar=1$) and describes the coupling strength between the field and the atom. We have also introduced the dimensionless momentum $r=k/\kappa$, the dimensionless cavity-length $L=\kappa l$, and the dimensionless one-photon detuning. In these figures we plot the variation of the dimensionless linewidth $D=\mathrm{Re}<\mu_n^{(1)}>/\gamma$ and the dimensionless frequency-shift $S=-\mathrm{Im}<\mu_n^{(1)}>/2\gamma$ versus the dimensionless cavity-length $L$ with $r, N_{\rm ex}, n_b, \delta$

and $\eta$ as parameters. For comparison we have also plotted the variation of the mean number of photons $< n >= \sum_{n=0}^{\infty} nP_n$ versus $L$. Now we discuss these figures in some detail.

Figure 2 is for the case of fast atoms ($r >> 1$) with $r = 100$. The minima in $< n >$ correspond to the trapping states. For the trapping states, the linewidth $D$ is significantly broadened. There is a small frequency-shift toward the blue side ($S$ has positive value). As a whole, the frequency-shift increases as $L$ increases, but there are some minima for the trapping states.

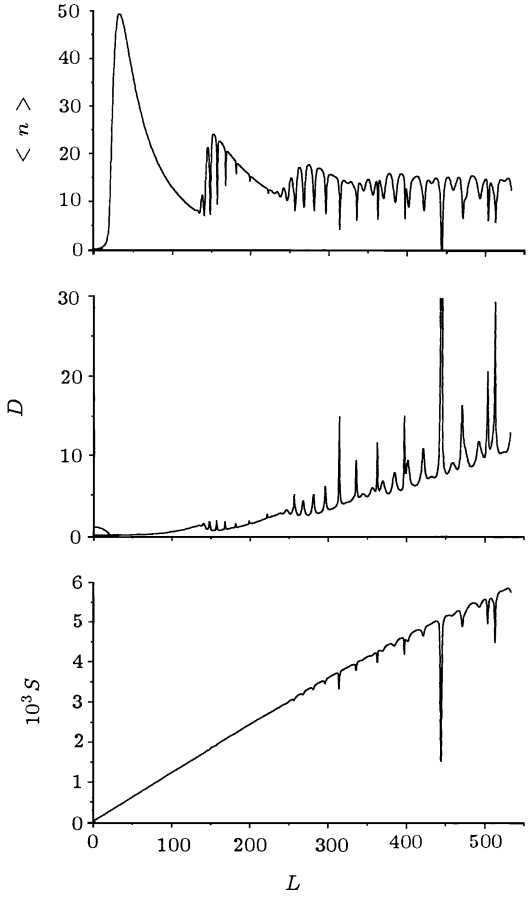



**Fig.2.** The variation of the mean number of photons $< n >$, the dimensionless linewidth $D$, and the dimensionless frequency-shift $S$ versus the dimensionless cavity-length $L$ for the fast-atom case with $r$=100, $\delta$=0, $\eta = 1$, $N_{\rm ex}$=50, and $n_b = 10^{-4}$.

Figure 3 is for the case of intermediate-velocity atoms ($r \approx 1$) with $r = 1$. With the increase of $L$, we find that $< n >$ first oscillates, then approaches a nearly constant value. $D$ increases as $L$ increases. There is a frequency shift toward the red side ($S$ has negative values) and the frequency-shift increases ($|S|$ increases) as $L$ increases.

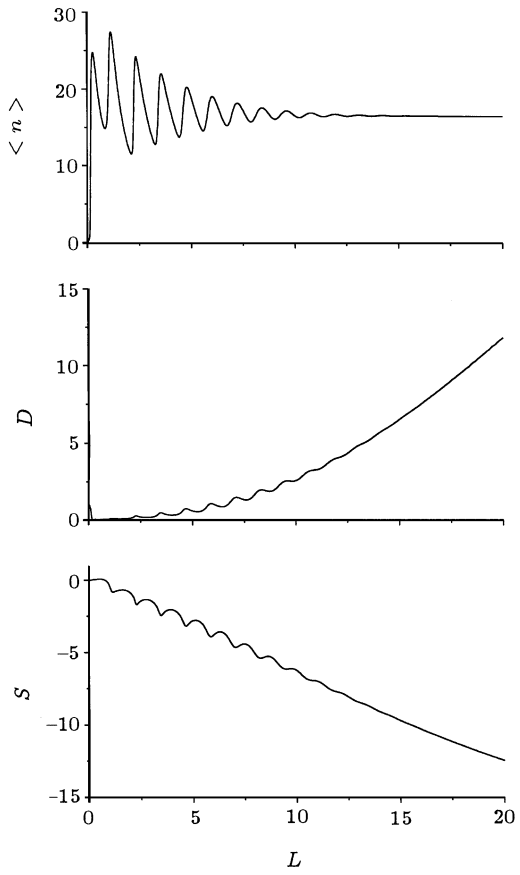



**Fig.3.** The same as Fig.2 but for the intermediate-velocity-atom case with $r = 1$.

Figure 4 is for the case of slow atoms ($r << 1$) with $r = 0.01$. The mean number of $< n >$ photons shows some sharp peaks and the maximum values at the peaks are about 1. This means that the cavity contains, at most, only one photon. For most values of the cavity-length $L$, we have $< n >\approx 0$. Corresponding to the peaks, the linewidth has large values and the frequency-shift changes its sign suddenly.

In order to compare with the two-level-atom case, we have done numerical calculations with $\eta$ changing from 0 to 1, and found some similarities and differences between the three-level-atom case ($\eta \neq 0$) and the two-level- atom case ($\eta = 0$). The curves look similar in these two cases, this is because here we

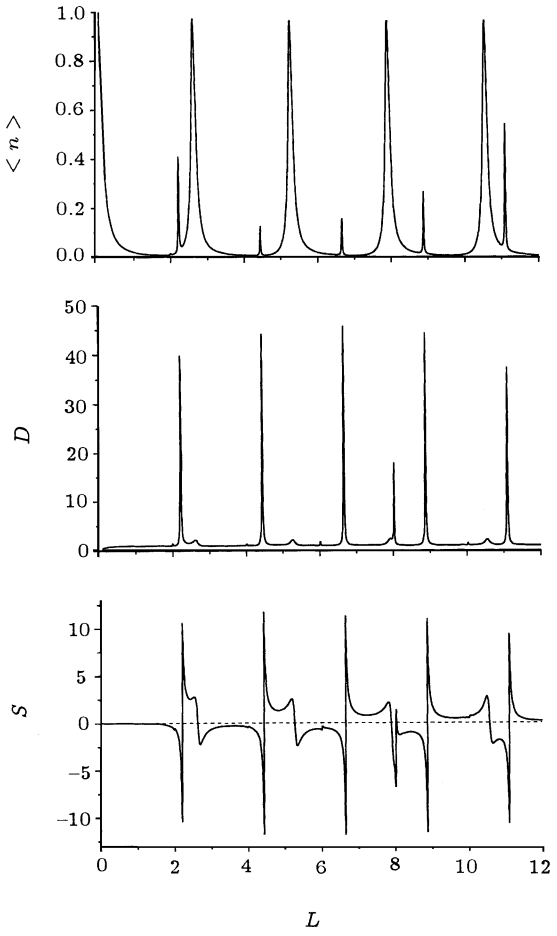



**Fig.4.** The same as Fig.2 but for the slow-atom case with $r = 0.01$.

consider only the situation in which the two lower atom levels are degenerate and the field has only one mode. The differences occur mainly in the oscillation "frequency". The oscillations of $< n >$, $D$, and $S$ become faster with increasing $\eta$. The reason for this is that there are two transition passages ($|a\rangle \leftrightarrow |b\rangle$ and $|a\rangle \leftrightarrow |c\rangle$) in the three-level-atom case, this makes the exchange of energy between the field and the atom become faster. We expect that more differences appear when we consider the case in which the two lower atom levels are not degenerate and the field has two modes. This problem will be studied in the future.

## IV. SUMMARY

In summary, the spectrum of the micromaser injected with $\Lambda$-type three-level atoms has been studied. We find that the spectrum has a Lorentzian lineshape and its central frequency has a shift. The linewidth and the frequency shift depend on various parameters, for example, the atomic center-of-mass velocity, the cavity-length, the one-photon detuning, the normalized atomic injection rate and the number of thermal photons. The effects of these parameters have been examined. We find that the spectrum shows very different features in the three different regimes, i.e. the fast-atom regime, the intermediate-velocity-atom regime, and the slow-atom regime.

## REFERENCES

[1] For a review, see G. Raithel, C. Wagner, H. Walther, L. M. Narducci and M.O.Scully, in Cavity Quantum Electrodynamics, edited by P. R. Berman ( Academic, Boston,1994), p.57.

[2] For laser-cooling techniques, see Laser Manipulation of Atoms and Ions, edited by E.Arimondo, W.D.Phillips, and F. Strumia (North-Holland, Amsterdam, 1992).

[3] M. O. Scully, G. M. Meyer and H. Walther, *Phys. Rev. Lett.,* **76**(1996),4144.

[4] G. M. Meyer, M. O. Scully and H. Walther, *Phys. Rev.,* **A56**(1997),4142.

[5] M. Loffler, G. M. Meyer, M. Schroder, M. O. Scully and H. Walther, *Phys. Rev.,* **A56**(1997),4153.

[6] M. Schroder, K. Vogel, W. P. Schleich, M. O. Scully and H. Walther, *Phys. Rev.,* **A56**(1997),4164.

[7] Z. M. Zhang and L. S. He, *Opt. Commun.,* **157**(1998),77.

[8] Z. M. Zhang, X. F. Li and S. K. Zhou, *Acta Physica Sinica (Overseas Edition),* **8**(1999),571.

[9] M. O. Scully, H. Walther, G. S. Agarwal, T. Quang and W. Schleich, *Phys. Rev.,* **A44**(1991),5992.